

# Stepwise Transformation of the Molecular Building Blocks in a Porphyrin-Encapsulating Metal–Organic Material

Zhenjie Zhang,<sup>†</sup> Lukasz Wojtas,<sup>†</sup> Mohamed Eddaoudi,<sup>†,‡</sup> and Michael J. Zaworotko<sup>\*,†</sup>

<sup>†</sup>Department of Chemistry, University of South Florida, 4202 East Fowler Avenue, CHE205, Tampa, Florida 33620, United States

<sup>‡</sup>Chemical Science Program, 4700 King Abdullah University of Science and Technology, Thuwal 23955-6900, Kingdom of Saudi Arabia

**S** Supporting Information

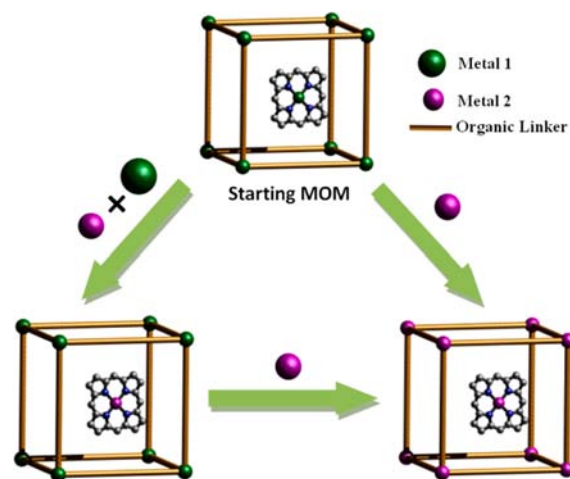
**ABSTRACT:** When immersed in solutions containing Cu(II) cations, the microporous metal–organic material **P11** ( $[\text{Cd}_4(\text{BPT})_4] \cdot [\text{Cd}(\text{C}_{44}\text{H}_{36}\text{N}_8)(\text{S})] \cdot [\text{S}]$ , BPT = biphenyl-3,4',5-tricarboxylate) undergoes a transformation of its  $[\text{Cd}_2(\text{COO})_6]^{2-}$  molecular building blocks (MBBs) into novel tetranuclear  $[\text{Cu}_4\text{X}_2(\text{COO})_6(\text{S})_2]$  MBBs to form **P11-Cu**. The transformation occurs in single-crystal to single-crystal fashion, and its stepwise mechanism was studied by varying the  $\text{Cd}^{2+}/\text{Cu}^{2+}$  ratio of the solution in which crystals of **P11** were immersed. **P11-16/1** (Cd in framework retained, Cd in encapsulated porphyrins exchanged) and other intermediate phases were thereby isolated and structurally characterized. **P11-16/1** and **P11-Cu** retain the microporosity of **P11**, and the relatively larger MBBs in **P11-Cu** permit a 20% unit cell expansion and afford a higher surface area and a larger pore size.

Porous metal–organic materials (MOMs) that incorporate reactive species (RS) such as metalloporphyrins,<sup>1</sup> metallosalens,<sup>2</sup> and polyoxometalates<sup>3</sup> are of topical interest because they can combine the physicochemical properties of the RS<sup>4</sup> with permanent porosity of the framework.<sup>5</sup> Such MOMs can thereby enable new approaches to gas storage,<sup>6</sup> separations,<sup>7</sup> luminescence, and catalysis,<sup>8</sup> including enzymatic catalysis.<sup>8b</sup> MOMs that incorporate RS can be divided into two subgroups: those with RS as an integral part of nodes/linkers (RSMOMs)<sup>9</sup> and those that encapsulate or host RS in cages (RS@MOMs).<sup>10</sup> Encapsulation may be achieved directly through synthesis<sup>11</sup> or via postsynthetic modification (PSM).<sup>12</sup> Metalloporphyrins are attractive RS because of their value as catalysts<sup>13</sup> and dyes,<sup>14</sup> and we recently reported the generation of porphyrin-encapsulating MOMs (porph@MOMs)<sup>15</sup> that exhibit PSM through metal ion exchange<sup>16</sup> or metal salt incorporation.<sup>17</sup> The availability of such porph@MOMs offers the opportunity to study their PSM systematically and evaluate its impact on their properties such as gas sorption, luminescence, and catalysis. In addition, PSM can afford new compounds that cannot be directly synthesized.

PSM involving metal exchange in molecular building blocks (MBBs) is now widely studied and tends to focus upon Cd- and Zn-containing MOMs<sup>18</sup> because of the relative lability of complexes of d<sup>10</sup> ions ( $\text{Cd}^{2+}$ ,  $\text{Zn}^{2+}$ , and  $\text{Hg}^{2+}$ ).<sup>19</sup> The metal exchange process is typically monitored using atomic absorption spectroscopy (AAS) and powder X-ray diffraction (PXRD), and examples where PSM has been followed using single-crystal X-

ray diffraction (SCXRD) are rare.<sup>16,20</sup> Since  $\text{Cd}^{2+}$  in cadmium porphyrins can be irreversibly exchanged with  $\text{Cu}^{2+}$ ,<sup>21</sup> the possibility of selective control of PSM in porph@MOMs exists if the MOM and the encapsulated RS exhibit different rates of exchange. In this work, we addressed such a situation through the study of crystals of porph@MOM-11 (**P11**), a Cd-sustained MOM that encapsulates CdTMPyP cations [ $\text{H}_2\text{TMPyP} = \text{meso-tetra}(N\text{-methyl-4-pyridyl})\text{porphine tetratosylate}$ ]. **P11** was immersed in methanol solutions of  $\text{Cd}^{2+}$  and/or  $\text{Cu}^{2+}$  to study how the  $\text{Cd}^{2+}/\text{Cu}^{2+}$  mole ratio impacts PSM. Scheme 1 shows how porph@MOMs might generally undergo complete or partial metal exchange through control of the ratio of two metal ions.

**Scheme 1. Metal Ion PSM in porph@MOMs: (i) Partial PSM with Metal 2 in the Presence of Both Metal 1 and 2 (Bottom Left); (ii) Complete Exchange with Metal 2 (Bottom Right)**



The reaction of biphenyl-3,4',5-tricarboxylic acid ( $\text{H}_3\text{BPT}$ )<sup>22</sup> and  $\text{Cd}(\text{NO}_3)_2$  with  $\text{H}_2\text{TMPyP}$  afforded **P11**, a microporous MOM in which encapsulated cationic porphyrins occupy alternating channels.<sup>17</sup> **P11** is based upon a 3,6-connected rtl net built from two 6-connected  $[\text{Cd}_2(\text{COO})_6]^{2-}$  MBBs [Figure 1a and Figure S1 in the Supporting Information (SI)]. As illustrated in Figure S1, one MBB is a distorted paddlewheel formed by seven-coordinate  $\text{Cd}^{2+}$  and the other is a more regular

Received: February 12, 2013

Published: April 2, 2013

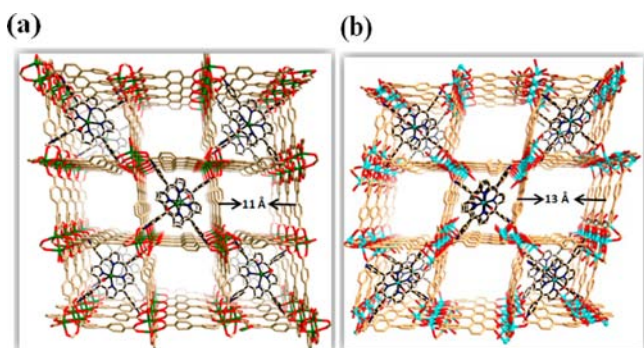


**Figure 1.** Crystal structures of (a) **P11** and (b) **P11-Cu** viewed down the crystallographic *a* axis.

paddlewheel formed by six-coordinate  $\text{Cd}^{2+}$ .  $\text{CdTMPyP}$  cations are alternately arranged in 1D channels, and the remaining channels are occupied by solvent molecules (Figure 1a). The anticipated lability of  $\text{Cd}^{2+}$  and the readily accessible pores of **P11** [permanent porosity, Brunauer–Emmett–Teller (BET) surface area =  $997 \text{ m}^2/\text{g}$ ] offer the potential for PSM through metal ion exchange. Indeed, when crystals of **P11** were immersed in 0.05 M  $\text{Cu}(\text{NO}_3)_2$  in MeOH for 10 days with refreshment of the solution three times, they were transformed into a new crystalline MOM, **P11-Cu** (Figure 1b), which suggested a single-crystal to single-crystal (SC-to-SC) process. Moreover, **P11-Cu** cannot be directly synthesized under the conditions used for PSM, making its formation by a dissolution and recrystallization process unlikely.<sup>18h</sup> AAS revealed complete exchange of the  $\text{Cd}^{2+}$  cations in **P11** with  $\text{Cu}^{2+}$ . SCXRD of **P11-Cu**,  $[\text{Cu}_8(\text{X})_4(\text{BPT})_4(\text{S})_8] \cdot [\text{NO}_3]_4 \cdot [\text{Cu}(\text{C}_{44}\text{H}_{36}\text{N}_8\text{S})] \cdot [\text{S}]$  ( $\text{S} = \text{MeOH}, \text{H}_2\text{O}; \text{X} = \text{CH}_3\text{O}^-, \text{OH}^-$ ), revealed a larger unit cell than in **P11**, with an associated unit cell volume expansion from  $3779.3(2)$  to  $4133.0(5) \text{ \AA}^3$  (Table S4 in the SI). This can be attributed to the transformation of the dimetallic  $[\text{Cd}_2(\text{COO})_6]^{2-}$  MBBs of **P11** into larger 6-connected tetrametallic  $[\text{Cu}_4\text{X}_2(\text{COO})_6(\text{S})_2]$  MBBs. To our knowledge, this type of transformation is unprecedented in MOM chemistry.

The use of synchrotron radiation enabled a structural study of the transformation of **P11** to **P11-Cu**. Comparison of the novel  $[\text{Cu}_4\text{X}_2(\text{COO})_6(\text{S})_2]$  MBB in **P11-Cu** with the starting MBB in **P11** (Figure 2) revealed that there are two crystallographically

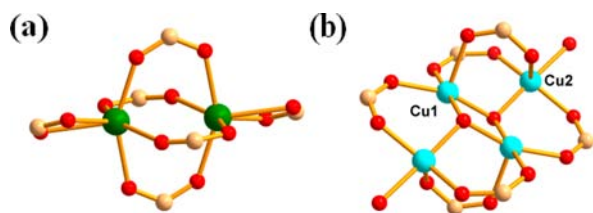


**Figure 2.** (a) Dinuclear  $\text{Cd}^{2+}$  MBB in **P11**. (b) Novel tetranuclear  $\text{Cu}^{2+}$  MBB in **P11-Cu**.

independent five-coordinate  $\text{Cu}^{2+}$  cations. The coordination environment of  $\text{Cu1}$  can be approximately described as trigonal-bipyramidal and consists of two  $\mu_3\text{-X}$  and three monodentate O atoms of bridging carboxylate moieties. The  $\text{Cu1-O}$  bond distances lie in the range  $1.928(4)$ – $2.210(4) \text{ \AA}$ , and the  $\text{O-Cu1-O}$  bond angles range from  $84.8(2)$  to  $177.9(2)^\circ$ .  $\text{Cu2}$  exhibits a geometry similar to that of  $\text{Cu1}$ : it is bonded to one  $\mu_3\text{-X}$ , three monodentate O atoms of bridging carboxylate moieties, and one solvent O atom; the  $\text{Cu2-O}$  bond distances range from

$1.929(4)$  to  $2.150(5) \text{ \AA}$ , and the  $\text{O-Cu2-O}$  bond angles range from  $82.5(2)$  to  $174.2(2)^\circ$ . The  $\mu_3\text{-X}$  moieties of the MBB are crystallographically disordered  $\text{OH}^-$  or  $\text{CH}_3\text{O}^-$  anions<sup>23</sup> with  $\text{Cu-O}$  distances of  $1.933(5)$ – $2.007(4) \text{ \AA}$ . The overall geometry of the MBB in **P11-Cu** can be described as pseudo-octahedral, and therefore, the MBB serves the same structure-directing/building role as the starting 6-connected MBB in **P11**. However, the distances between the C atoms of opposite carboxylate moieties range from  $6.05$  to  $7.63 \text{ \AA}$  in **P11-Cu**, versus the corresponding values of  $5.45$ – $8.61 \text{ \AA}$  in **P11**. **P11-Cu** therefore exhibits larger 1D channels than **P11**, with the pore size (i.e., the distance between opposite pore walls minus the van der Waals radii) expanding from ca.  $11.0$  to ca.  $13.0 \text{ \AA}$ . In addition, the encapsulated  $\text{CdTMPyP}$  cations were converted into  $\text{CuTMPyP}$  cations, as verified by the solution-state UV–vis spectrum of the dissolved crystals (Figure S2). Attempts to prepare **P11-Cu** directly by reaction of Cu salts with  $\text{H}_3\text{BPT}$  were unsuccessful.

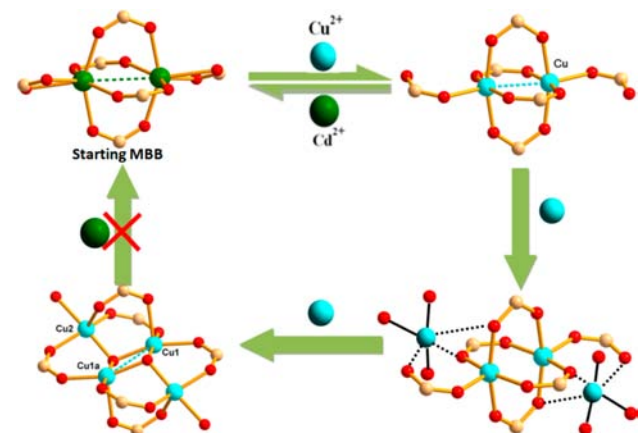
The transformation of **P11** to **P11-Cu** is not readily reversible, as AAS analysis after **P11-Cu** had been immersed in 0.05 M  $\text{Cd}(\text{NO}_3)_2$  in MeOH for 10 days revealed that almost no  $\text{Cu}^{2+}$  was exchanged with  $\text{Cd}^{2+}$  (Table S5). This observation contrasts with that of Kim and co-workers.<sup>20</sup> The bond distances and geometries in **P11** and **P11-Cu** were consistent with the expected values, as analysis of the Cambridge Structural Database (ConQuest version 1.14, Aug 2012 update<sup>24</sup>) revealed that  $\text{Cd}^{2+}$  favors six- or seven-coordinate environments with  $\text{Cd-O}$  bond distances of ca.  $2.28 \text{ \AA}$  whereas  $\text{Cu}^{2+}$  tends to favor five- or six-coordinate environments with  $\text{Cu-O}$  bond distances of ca.  $1.96 \text{ \AA}$ .

We further studied the metal exchange process by treating **P11** with  $\text{Cd}(\text{NO}_3)_2/\text{Cu}(\text{NO}_3)_2$  in MeOH solutions in which the total metal ion concentration was fixed at 0.05 M. After immersion in a variety of such solutions for 10 days (with refreshment of the solution three times), the resulting crystals were harvested and characterized. When the  $\text{Cd}^{2+}/\text{Cu}^{2+}$  ratio was 2:1, crystals of **P11-2/1** with a unit cell similar to that of **P11-Cu** were obtained (Table S4). AAS and UV–vis spectroscopy confirmed that  $\text{Cd}^{2+}$  was fully exchanged with  $\text{Cu}^{2+}$  in both the framework and the porphyrin moiety (Table S5 and Figure S2). However, when  $\text{Cd}^{2+}/\text{Cu}^{2+}$  ratios of 4:1 and 8:1 were used, the resulting phases (**P11-4/1** and **P11-8/1**, respectively) were observed to exhibit unit cell parameters close to those of **P11**. SCXRD indicated that the  $\text{Cd}^{2+}$  paddlewheels were only partially exchanged with  $\text{Cu}^{2+}$ . However, UV–vis spectroscopy indicated that the  $\text{Cd}^{2+}$  cations in  $\text{CdTMPyP}$  were fully exchanged with  $\text{Cu}^{2+}$  cations. AAS revealed that 86.6 and 77.5% of the  $\text{Cd}^{2+}$  cations in the MBBs of **P11-4/1** and **P11-8/1**, respectively, were exchanged with  $\text{Cu}^{2+}$ . To ascertain whether or not **P11-4/1** and **P11-8/1** could be reversibly exchanged, crystals were immersed in 0.05 M  $\text{Cd}(\text{NO}_3)_2$  in MeOH for 10 days. Analysis of the resulting crystals by AAS showed that the amount of exchanged  $\text{Cu}^{2+}$  cations in the MBBs had decreased to 55 and 46%, respectively. UV–vis spectroscopy indicated that the  $\text{Cu}^{2+}$  cations of the  $\text{CuTMPyP}$  moieties were not exchanged over the 10 day period (Figure S2). These observations imply that metal exchange can be reversible in partially exchanged MBBs but is irreversible in  $\text{CuTMPyP}$  moieties. When the  $\text{Cd}^{2+}/\text{Cu}^{2+}$  ratio was increased to 16/1 to afford crystals of **P11-16/1**, the unit cell was measured to be that of **P11** and structure refinement showed no evidence of exchange of  $\text{Cd}^{2+}$  with  $\text{Cu}^{2+}$  in the MBBs. However, the  $\text{Cd}^{2+}$  ions in the  $\text{CdTMPyP}$  moieties were completely exchanged, as verified by SCXRD and UV–vis spectroscopy (Figure S2). AAS suggested that <4% of the  $\text{Cd}^{2+}$

was exchanged with  $\text{Cu}^{2+}$  in the  $\text{Cd}^{2+}$  MBBs. Further immersion of crystals of **P11-16/1** into 0.05 M  $\text{Cd}(\text{NO}_3)_2$  for 10 days did not lead to exchange of the  $\text{Cu}^{2+}$  cations in  $\text{CuTMPyP}$ , as verified by UV-vis spectroscopy and AAS. In addition, attempts to prepare **P11-16/1** directly by reactions of  $\text{Cd}(\text{NO}_3)_2$  with  $\text{H}_3\text{BPT}$  and  $\text{CuTMPyP}$  were unsuccessful.

To elucidate further the formation of  $[\text{Cu}_4\text{X}_2(\text{COO})_6(\text{S})_2]$  MBBs in **P11-Cu**, **P11-8/1** was immersed in 0.05 M  $\text{Cu}(\text{NO}_3)_2$  for 10 days. The harvested crystals exhibited the unit cell parameters  $a = 10.715(5) \text{ \AA}$ ,  $b = 18.735(5) \text{ \AA}$ ,  $c = 21.170(5) \text{ \AA}$ ,  $\alpha = 89.453(5)^\circ$ ,  $\beta = 88.294(5)^\circ$ ,  $\gamma = 85.071(5)^\circ$ , and  $V = 4232(2) \text{ \AA}^3$ , suggesting that the transformation to **P11-Cu** had occurred. As revealed in Scheme 2,  $\text{Cd}^{2+}$  paddlewheels were partially

#### Scheme 2. Possible Pathway to $[\text{Cu}_4\text{X}_2(\text{COO})_6(\text{S})_2]$ MBBs Starting from $[\text{Cd}_2(\text{COO})_6]^{2-}$ MBBs As Determined by Metal Ion Exchange and SCXRD



exchanged to form dinuclear  $\text{Cu}^{2+}$  paddlewheels in which the metal-metal distance had decreased from ca. 3.33  $\text{\AA}$  in **P11** to ca. 3.25  $\text{\AA}$  in **P11-8/1**. These  $\text{Cu}^{2+}$  paddlewheels contain monodentate carboxylate ligands in the axial sites. When **P11-8/1** was treated with a more concentrated solution of  $\text{Cu}^{2+}$ , the  $\text{Cu}^{2+}$  paddlewheels can possibly bind two solvated  $\text{Cu}^{2+}$  cations in such a manner that they are chelated by three carboxylate O atoms to form a  $\text{Cu}_4$  intermediate (Scheme 2, bottom right). This  $\text{Cu}_4$  intermediate is consistent with our recent observation that salt addition of  $\text{Ba}^{2+}$  cations to Cd paddlewheels can occur via coordination through three carboxylate O atoms in **porph(Cl<sup>-</sup>)@MOM-11(Ba<sup>2+</sup>)** (Figure S3).<sup>17</sup> The  $\text{Cu}_4$  intermediate subsequently undergoes a rearrangement to form the tetrametallic  $[\text{Cu}_4\text{X}_2(\text{COO})_6(\text{S})_2]$  MBB that sustains **P11-Cu**.

Thermogravimetric analysis (TGA) revealed that **P11-Cu** and **P11-16/1** exhibit approximately the same weight loss (ca. 13.5%) below 110  $^\circ\text{C}$  and thereafter are stable to 250 and 300  $^\circ\text{C}$ , respectively (Figure S4). Supercritical  $\text{CO}_2$ <sup>25</sup> was used to activate the samples for gas sorption measurements. The porosity of the PSM product **P11-16/1** (BET surface area = 1009  $\text{m}^2/\text{g}$ , Langmuir surface area = 1127  $\text{m}^2/\text{g}$ ) is comparable to that of **P11** (BET surface area = 997  $\text{m}^2/\text{g}$ , Langmuir surface area = 1096  $\text{m}^2/\text{g}$ ), and **P11-16/1** has a  $\text{N}_2$  uptake of 265  $\text{cm}^3$  (STP)/g at 77 K and  $P/P_0 = 0.95$  (Figure 3a). The slightly higher surface area of **P11-16/1** can be ascribed to its slightly lower density (1.024  $\text{g}/\text{cm}^3$  vs 1.050  $\text{g}/\text{cm}^3$  for **P11**). At 77 K and  $P/P_0 = 0.95$ , **P11-Cu** was found to sorb a relatively large amount of  $\text{N}_2$  [345  $\text{cm}^3$  (STP)/g]. The calculated BET and Langmuir surface areas were 1251 and 1406  $\text{m}^2/\text{g}$ , respectively. The pore size distribution

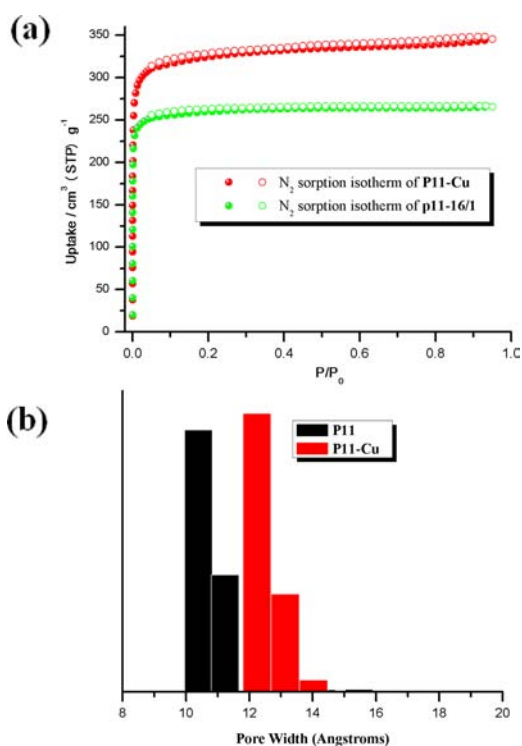


**Figure 3.** (a)  $\text{N}_2$  sorption isotherms at 77 K for **P11-16/1** and **P11-Cu**. (b) Pore size distributions for **P11** and **P11-Cu**.

determined using  $\text{N}_2$  revealed that **P11-Cu** has micropores with sizes of ca. ~13  $\text{\AA}$  (vs 11  $\text{\AA}$  in **P11**; Figure 3b), consistent with the crystal structure.  $\text{CO}_2$  sorption was also studied, and **P11-Cu** was found to exhibit smaller uptake than **P11** (49 vs 59  $\text{cm}^3/\text{g}$ , respectively) at 298 K and 1 atm. This observation suggests that the isosteric heat ( $Q_{\text{st}}$ ) of  $\text{CO}_2$  adsorption is lower for **P11-Cu** than for **P11**. Indeed, calculations based on  $\text{CO}_2$  isotherms collected at 273 and 298 K (Figures S5 and S6) revealed that the initial  $Q_{\text{st}}$  for **P11-Cu** is 29.8 kJ/mol, versus 30.3 kJ/mol for **P11** (Figure S7). A decrease in  $Q_{\text{st}}$  for  $\text{CO}_2$  as the pore size increases has been seen in other MOMs.<sup>26,27</sup> The  $Q_{\text{st}}$  for  $\text{CO}_2$  in turn impacts the selectivity for  $\text{CO}_2$ . IAST<sup>28</sup> calculations based on the experimental  $\text{CO}_2$  and  $\text{CH}_4$  isotherms at 298 K are presented in Figure S8. **P11-Cu** has a lower selectivity for  $\text{CO}_2$  versus  $\text{CH}_4$  than the parent **P11** over the entire studied pressure range. The initial selectivity of **P11-Cu** was calculated to be 5.0 versus 7.1 for **P11**. This observation is also consistent with other studies on the effect of pore size on gas sorption.<sup>27</sup>

In conclusion, the  $\text{Cd}^{2+}$ -based **porph@MOM P11** is a versatile platform that can undergo metal ion exchange with  $\text{Cu}^{2+}$  in an SC-to-SC fashion. The use of mixed metal salt solutions ( $\text{Cu}^{2+}/\text{Cd}^{2+}$ ) with varying ratios of metal salts enabled a systematic study of the metal exchange process in **P11**, which showed that at one extreme only the  $\text{Cd}^{2+}$  porphyrin moieties undergo metal ion exchange, whereas at the other extreme the ions in both the framework and the porphyrin moieties are fully exchanged. In addition, for the first time we have observed a phenomenon in which the MBBs of the parent compound **P11** are transformed from a dimetallic MBB to a larger, previously uncommon tetrametallic MBB, thereby increasing unit cell size, pore size, and surface area.

## ■ ASSOCIATED CONTENT

## ■ Supporting Information

Crystal data (CIF); UV–vis, TGA, and PXRD data; supplemental structure pictures; and CO<sub>2</sub> adsorption isotherms, Q<sub>st</sub> plots, and selectivity plots. This material is available free of charge via the Internet at <http://pubs.acs.org>.

## ■ AUTHOR INFORMATION

## Corresponding Author

xtal@usf.edu

## Notes

The authors declare no competing financial interest.

## ■ ACKNOWLEDGMENTS

This work was supported by Award FIC/2010/06 from King Abdullah University of Science and Technology. The data for P11-Cu were collected at the Advanced Photon Source on beamline 15ID-C of ChemMatCARS Sector 15, which is principally supported by the National Science Foundation/Department of Energy under Grant NSF/CHE-0822838. The Advanced Photon Source is supported by the U.S. Department of Energy, Office of Science, Office of Basic Energy Sciences, under Contract DE-AC02-06CH11357.

## ■ REFERENCES

- (1) Lee, S. J.; Hupp, J. T. *Coord. Chem. Rev.* **2006**, *250*, 1710.
- (2) Xuan, W.; Zhang, M.; Liu, Y.; Chen, Z.; Cui, Y. *J. Am. Chem. Soc.* **2012**, *134*, 6904.
- (3) Song, J.; Luo, Z.; Britt, D. K.; Furukawa, H.; Yaghi, O. M.; Hardcastle, K. I.; Hill, C. L. *J. Am. Chem. Soc.* **2011**, *133*, 16839.
- (4) (a) Juan-Alcañiz, J.; Gascon, J.; Kapteijn, F. *J. Mater. Chem.* **2012**, *22*, 10102. (b) Beletskaya, I.; Tyurin, V. S.; Tsvadze, A. Y.; Guillard, R.; Stern, C. *Chem. Rev.* **2009**, *109*, 1659. (c) Stracke, J. J.; Finke, R. G. *J. Am. Chem. Soc.* **2011**, *133*, 14872. (d) Breslow, R.; Brown, A. B.; McCullough, R. D.; White, P. W. *J. Am. Chem. Soc.* **1989**, *111*, 4518.
- (5) Furukawa, H.; Ko, N.; Go, Y. B.; Aratani, N.; Choi, S. B.; Choi, E.; Yazaydin, A. O.; Snurr, R. Q.; O’Keeffe, M.; Kim, J.; Yaghi, O. M. *Science* **2010**, *239*, 424.
- (6) (a) Choi, E.-Y.; Wray, C. A.; Hu, C.; Choe, W. *CrystEngComm* **2009**, *11*, 553. (b) Shultz, A. M.; Farha, O. K.; Hupp, J. T.; Nguyen, S. T. *J. Am. Chem. Soc.* **2009**, *131*, 4204.
- (7) Wang, X.-S.; Meng, L.; Cheng, Q.; Kim, C.; Wojtas, L.; Chrzanowski, M.; Chen, Y.-S.; Zhang, X. P.; Ma, S. *J. Am. Chem. Soc.* **2011**, *133*, 16322.
- (8) (a) Lee, C. Y.; Farha, O. K.; Hong, B. J.; Sarjeant, A. A.; Nguyen, S. T.; Hupp, J. T. *J. Am. Chem. Soc.* **2011**, *133*, 15858. (b) Lykourinou, V.; Chen, Y.; Wang, X.-S.; Meng, L.; Hoang, T.; Ming, L.-J.; Musselman, R. L.; Ma, S. *J. Am. Chem. Soc.* **2011**, *133*, 10382.
- (9) (a) Suslick, K. S.; Bhyrappa, P.; Chou, J. H.; Kosal, M. E.; Nakagaki, S.; Smithenry, D. W.; Wilson, S. R. *Acc. Chem. Res.* **2005**, *38*, 283. (b) Das, M. C.; Guo, Q.; He, Y.; Kim, J.; Zhao, C.-G.; Hong, K.; Xiang, S.; Zhang, Z.; Thomas, K. M.; Krishna, R.; Chen, B. *J. Am. Chem. Soc.* **2012**, *134*, 8703. (c) Goldberg, I. *Chem. Commun.* **2005**, 1243. (d) Abrahams, B. F.; Hoskins, B. F.; Michail, D. M.; Robson, R. *Nature* **1994**, *369*, 727. (e) Zimmerman, S. C.; Wendland, M. S.; Rakow, N. A.; Suslick, K. S. *Nat. Mater.* **2002**, *1*, 118. (f) Shultz, A. M.; Sarjeant, A. A.; Farha, O. K.; Hupp, J. T.; Nguyen, S. T. *J. Am. Chem. Soc.* **2011**, *133*, 13252.
- (10) (a) Ono, K.; Yoshizawa, M.; Kato, T.; Watanabe, K.; Fujita, M. *Angew. Chem., Int. Ed.* **2007**, *46*, 1803. (b) Alkordi, M. H.; Liu, Y.; Larsen, R. W.; Eubank, J. F.; Eddaoudi, M. *J. Am. Chem. Soc.* **2008**, *130*, 12639. (c) Larsen, R. W.; Wojtas, L.; Perman, J.; Musselman, R. L.; Zaworotko, M. J.; Vetrovile, C. M. *J. Am. Chem. Soc.* **2011**, *133*, 10356. (d) Larsen, R. W.; Miksovská, J.; Musselman, R. L.; Wojtas, L. *J. Phys. Chem. A* **2011**, *115*, 11519. (e) Ma, F.-J.; Liu, S.-X.; Sun, C.-Y.; Liang, D.-D.; Ren, G.-J.; Wei, F.; Chen, Y.-G.; Su, Z.-M. *J. Am. Chem. Soc.* **2011**, *133*, 4178.
- (11) Sun, C.-Y.; Liu, S.-X.; Liang, D.-D.; Shao, K.-Z.; Ren, Y.-H.; Su, Z.-M. *J. Am. Chem. Soc.* **2009**, *131*, 1883.
- (12) Kockrick, E.; Lescouet, T.; Kudrik, E. V.; Sorokin, A. B.; Farrusseng, D. *Chem. Commun.* **2011**, *47*, 1562.
- (13) Lu, H.; Zhang, X. P. *Chem. Soc. Rev.* **2011**, *40*, 1899.
- (14) Walter, M. G.; Rudine, A. B.; Wamser, C. C. *J. Porphyrins Phthalocyanines* **2010**, *14*, 759.
- (15) Zhang, Z.; Zhang, L.; Wojtas, L.; Eddaoudi, M.; Zaworotko, M. J. *J. Am. Chem. Soc.* **2012**, *134*, 928.
- (16) Zhang, Z.; Zhang, L.; Wojtas, L.; Nugent, P.; Eddaoudi, M.; Zaworotko, M. J. *J. Am. Chem. Soc.* **2012**, *134*, 924.
- (17) Zhang, Z.; Gao, W.-Y.; Wojtas, L.; Ma, S.; Eddaoudi, M.; Zaworotko, M. J. *Angew. Chem., Int. Ed.* **2012**, *51*, 9330.
- (18) (a) Prasad, T. K.; Hong, D. H.; Suh, M. P. *Chem.—Eur. J.* **2010**, *16*, 14043. (b) Zhao, J.; Mi, L.; Hu, J.; Hou, H.; Fan, Y. *J. Am. Chem. Soc.* **2008**, *130*, 15222. (c) Huang, S.; Li, X.; Shi, X.; Hou, H.; Fan, Y. *J. Mater. Chem.* **2010**, *20*, 5695. (d) Cohen, S. M. *Chem. Rev.* **2012**, *112*, 970. (e) Zhang, Z.-J.; Shi, W.; Niu, Z.; Li, H.-H.; Zhao, B.; Cheng, P.; Liao, D.-Z.; Yan, S.-P. *Chem. Commun.* **2011**, *47*, 6425. (f) Mukherjee, G.; Biradha, K. *Chem. Commun.* **2012**, *48*, 4293. (g) Brozek, C. K.; Dincă, M. *Chem. Sci.* **2012**, *3*, 2110. (h) Kim, M.; Cahill, J. F.; Fei, H.; Prather, K. A.; Cohen, S. M. *J. Am. Chem. Soc.* **2012**, *134*, 18082. (i) Song, X.; Kim, T. K.; Kim, H.; Kim, D.; Jeong, S.; Moon, H. R.; Lah, M. S. *Chem. Mater.* **2012**, *24*, 3065. (j) Wang, X.-S.; Chrzanowski, M.; Wojtas, L.; Chen, Y.-S.; Ma, S. *Chem.—Eur. J.* **2013**, *19*, 3297. (k) Cairns, A. J.; Perman, J. A.; Wojtas, L.; Kravtsov, V. Ch.; Alkordi, M. H.; Eddaoudi, M.; Zaworotko, M. J. *J. Am. Chem. Soc.* **2008**, *130*, 1560.
- (19) *Coordination Chemistry*; Gispert, J. R., Ed.; Wiley-VCH: Weinheim, Germany, 2008.
- (20) Das, S.; Kim, H.; Kim, K. *J. Am. Chem. Soc.* **2009**, *131*, 3814.
- (21) (a) Stinson, C.; Hambricht, P. *J. Am. Chem. Soc.* **1977**, *99*, 2357. (b) *The Porphyrin Handbook*; Kadish, K. M., Smith, K. M., Guillard, R.; Eds.; Academic Press: San Diego, 2000–2003.
- (22) (a) Wong-Foy, A. G.; Lebel, O.; Matzger, A. J. *J. Am. Chem. Soc.* **2007**, *129*, 15740. (b) Schnobrich, J. K.; Lebel, O.; Cychoz, K. A.; Dailly, A.; Wong-Foy, A. G.; Matzger, A. J. *J. Am. Chem. Soc.* **2010**, *132*, 13941.
- (23) (a) Murugesu, M.; Anson, C. E.; Powell, A. K. *Chem. Commun.* **2002**, 1054. (b) Allan, P. K.; Xiao, B.; Teat, S. J.; Knight, J. W.; Morris, R. E. *J. Am. Chem. Soc.* **2010**, *132*, 3605.
- (24) Allen, F. *Acta Crystallogr.* **2002**, *B58*, 380.
- (25) (a) Nelson, A. P.; Farha, O. K.; Mulfort, K. L.; Hupp, J. T. *J. Am. Chem. Soc.* **2009**, *131*, 458. (b) Farha, O. K.; Hupp, J. T. *Acc. Chem. Res.* **2010**, *43*, 1166.
- (26) Mulfort, K. L.; Wilson, T. M.; Wasielewski, M. R.; Hupp, J. T. *Langmuir* **2009**, *25*, 503.
- (27) (a) Burd, S. D.; Ma, S.; Perman, J. A.; Sikora, B. J.; Snurr, R. Q.; Thallapally, P. K.; Tian, J.; Wojtas, L.; Zaworotko, M. J. *J. Am. Chem. Soc.* **2012**, *134*, 3663. (b) Nugent, P.; Belmabkhout, Y.; Burd, S. D.; Cairns, A. J.; Luebke, R.; Forrest, K.; Pham, T.; Ma, S.; Space, B.; Wojtas, L.; Eddaoudi, M.; Zaworotko, M. J. *Nature* **2013**, *495*, 80.
- (28) Bae, Y.-S.; Mulfort, K. L.; Frost, H.; Ryan, P.; Punnathanam, S.; Broadbelt, L. J.; Hupp, J. T.; Snurr, R. Q. *Langmuir* **2008**, *24*, 8592.